JACS
JOURNAL OF THE AMERICAN CHEMICAL SOCIETY
pubs.acs.org/JACS
Article

Rationally Designing the Supramolecular Interfaces of Nanoparticle Superlattices with Multivalent Polymers

Carl J. Thrasher,[¶] Fei Jia, Daryl W. Yee, Joshua M. Kubiak, Yuping Wang, Margaret S. Lee, Michika Onoda, A. John Hart, and Robert J. Macfarlane*

Cite This: J. Am. Chem. Soc. 2024, 146, 11532−11541
Read Online

ACCESS | Metrics & More | Article Recommendations | Supporting Information

ABSTRACT: In supramolecular materials, multiple weak binding groups can act as a single collective unit when confined to a localized volume, thereby producing strong but dynamic bonds between material building blocks. This principle of multivalency provides a versatile means of controlling material assembly, as both the number and the type of supramolecular moieties become design handles to modulate the strength of intermolecular interactions. However, in materials with building blocks significantly larger than individual supramolecular moieties (e.g., polymer or nanoparticle scaffolds), the degree of multivalency is difficult to predict or control, as sufficiently large scaffolds inherently preclude separated supramolecular moieties from interacting. Because molecular models commonly used to examine supramolecular interactions are intrinsically unable to examine any trends or emergent behaviors that arise due to nanoscale scaffold geometry, our understanding of the thermodynamics of these massively multivalent systems remains limited. Here we address this challenge via the coassembly of polymer-grafted nanoparticles and multivalent polymers, systematically examining how multivalent scaffold size, shape, and spacing affect their collective thermodynamics. Investigating the interplay of polymer structure and supramolecular group stoichiometry reveals complicated but rationally describable trends that demonstrate how the supramolecular scaffold design can modulate the strength of multivalent interactions. This approach to self-assembled supramolecular materials thus allows for the manipulation of polymer−nanoparticle composites with controlled thermal stability, nanoparticle organization, and tailored meso- to microscopic structures. The sophisticated control of multivalent thermodynamics through precise modulation of the nanoscale scaffold geometry represents a significant advance in the ability to rationally design complex hierarchically structured materials via self-assembly.

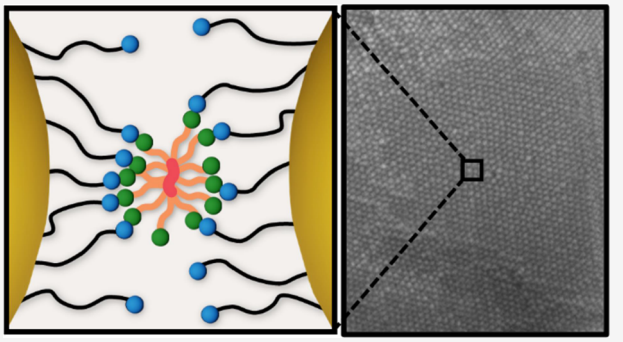

INTRODUCTION

Multivalent supramolecular interactions are commonly employed in the synthesis of complex materials, as they provide precision and versatility in the bonding interactions that govern material organization.[1−5] Tethering multiple weak supramolecular binding groups to common scaffold results in collective bonding interactions that are strong and permanent, even though individual supramolecular bonds remain dynamic.[6,7] The strength and specificity of multivalent bonds can therefore be tuned by changing the composition and number of constituent supramolecular interactions.[8,9] Significant advancement in materials design and supramolecular chemistry has emerged from fundamental studies of multivalent thermodynamics in molecular model systems, permitting the rational design of hydrogels, catalysts, sensors, and other functional materials.[10−17]

However, multivalent scaffolds consisting of macromolecules and nanostructures can possess 10s, 100s, or even 1000s of individual binding groups, and thus their multivalent behaviors are potentially governed by a more complex system of organized supramolecular interactions.[18−23] Indeed, once a multivalent scaffold becomes sufficiently massive, a new design parameter emerges that cannot be examined with molecular models—the relative locations of the supramolecular binding groups across the scaffold.[24−29] Because supramolecular moieties must be in close proximity to bond, the positions of individual groups affect how readily they can interact with one another, and therefore this geometric parameter can significantly affect multivalency. Early investigations into both multivalent polymer- and nanoparticle-based building blocks have measured phenomena that are controlled by (or inherently arise from) nanoscale scaffold geometry and bond flexibility, including multivalent bond strengths that increase

Received: February 21, 2024
Revised: April 1, 2024
Accepted: April 2, 2024
Published: April 15, 2024

https://doi.org/10.1021/jacs.4c02617
J. Am. Chem. Soc. 2024, 146, 11532−11541

asynchronously with increasing scaffold size, anisotropic or self-limiting growth of particle assemblies, and even entropy-driven reorganization of a scaffold's shape.[18,30−33] These examples demonstrate the importance of considering supramolecular chemistry from a hierarchical, "systems" approach where both the molecular and nanoscale geometries become interdependent factors affecting structure−property relationships.[34] Despite the importance of nanoscale geometry in dictating multivalent thermodynamics, this design parameter is challenging to analyze, as the emergent behaviors it induces in supramolecular systems cannot be fully understood simply by summing the effects of multiple individual molecular contributions. Therefore, better understanding and control of thermodynamic behaviors within these massively multivalent systems promises exciting opportunities for materials design but requires efforts to develop fundamental principles that apply to a range of polymer and nanoparticle systems.

Here, we present a multivalent system in which the thermodynamics of supramolecular assembly can be rationally controlled as a function of the nanoscale geometry of their interactions. Specifically, the multivalent interface between nanoparticle building blocks is mediated by macromolecular binders such that polymer size, shape, and functional group density act as design handles to organize the distribution of supramolecular binding groups. We show that this "brick and mortar" strategy[35−37] enables fundamental understanding of supramolecular thermodynamics in massively multivalent systems, permits assembly and tuning of single-crystal nanoparticle superlattices, and facilitates coalescence of multiple crystallites via paracrystalline distortion coordinated by supramolecular groups across micron-scale interfaces. These results demonstrate a "systems materials science" approach to supramolecular materials synthesis, where design parameters at the molecular, nano-, and microscales are interdependent handles to control the thermodynamics, hierarchical structures, and assembly behaviors of complex supramolecular systems.

RESULTS AND DISCUSSION

We have recently developed a suite of synthetically addressable building blocks termed "Nanocomposite Tectons" (NCTs) that use multivalent supramolecular interactions to enable the synthesis of hierarchical materials.[38−43] NCTs consist of inorganic nanoparticles coated with 100s or 1000s of polymer brushes, where each polymer chain is tipped with one-half of a binary supramolecular pair. When solutions of NCTs with complementary binding groups are mixed and thermally annealed, the particles are assembled into ordered superlattices. The size and composition of polymer and nanoparticle components, as well as the number of supramolecular binding groups per NCT, can be easily adjusted to tune the strength of the multivalent NCT−NCT bonds.

However, despite each particle containing ∼1000 supramolecular recognition groups, the enthalpy of multivalent NCT−NCT bonds is generally only ∼10 to 20 times greater than that of an individual supramolecular complex. This observation is a strong indication that massively multivalent NCT scaffolds cannot be understood as linear summations of their constituent molecular components. Prior work attributed this capping of multivalent enthalpy to the "bundling" of supramolecular groups within NCT−NCT connections constraining bond exchange such that each NCT−NCT interface was not a single multivalent system, but rather a collection of multiple discrete multivalent binding units.[18] That is, even though the interface between two NCTs might contain 100s of supramolecular binding groups, individual groups can only form thermodynamically favored connections with the complementary groups in their immediate vicinity (i.e., a local "bundle"). Experimental measurement and simulation showed that factors such as nanoparticle core size, polymer length, and polymer grafting density affected how supramolecular groups self-organized at the nanoscale interface between bonded NCTs and that this in turn could be used to control the crystallographic symmetry of assembled NCT superlattices.

Despite the profound impact of bundling on NCT assembly, it is difficult to see how the multivalency number of an NCT−NCT bond could be intentionally controlled or how generalizable design principles could be developed to predict thermodynamic properties over a broader range of polyvalent nanoscale systems. We hypothesize that these goals can be achieved using polymer binders to directly mediate multivalent binding between NCT particles. Rather than combining complementary NCT pairs, polymer binders permit a "brick and mortar" approach to multivalent assembly, where the multivalency number is directly controlled by adjusting polymer binder design (e.g., polymer molecular weights, recognition group densities, and backbone architectures) (Figure 1). This allows for a more modular and synthetically

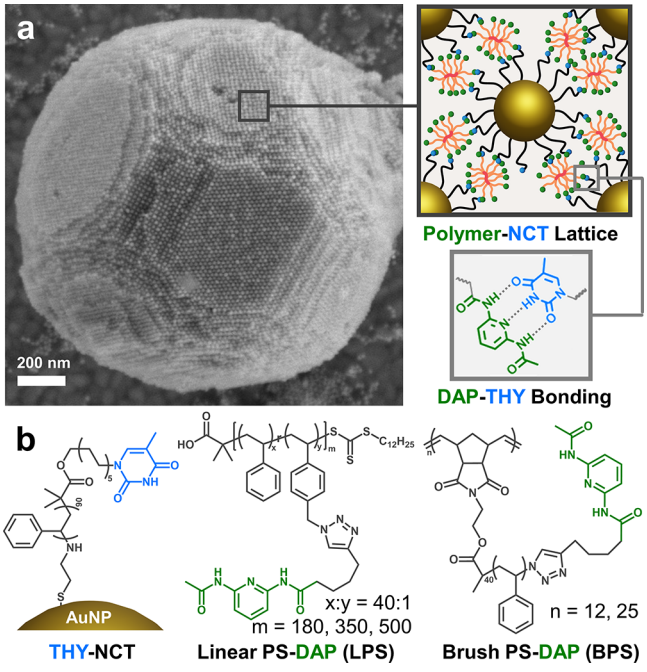

Figure 1. Composition of polymer−NCTs. (a) Scanning electron microscopy (SEM) image of a polymer−NCT crystal assembled with DAP−THY recognition complexes, schematically depicted at the right. (b) Chemical structures and associated depictions of THY−NCTs and DAP functionalized polymers used for assembly. All gold nanoparticle cores are ∼18 nm in diameter.

addressable approach to material assembly that provides insight into multivalent thermodynamics for a broad range of multivalent scaffolds.

The polymer binders used here include linear polystyrenes (LPS) and brush polystyrenes (BPS) modified with diaminopyridine (DAP) groups; these polymers and their nomenclature are listed in Table 1. To better enable comparison between systems, polymers were prepared with

https://doi.org/10.1021/jacs.4c02617
J. Am. Chem. Soc. 2024, 146, 11532−11541

Table 1. Characteristics of the Polymers Used in This Study

polymer	M_n (kDa)	$Đ$	DAP$_n$ (THY$_n$)
LPS-12	50.0	1.14	12
LPS-8*	50.0	1.14	8
LPS-8	35.9	1.15	8
LPS-4	18.2	1.08	4
BPS-25	112.3	1.60	25
BPS-12	51.2	1.53	12
NCT-THY	9.1[a]	1.04	(~800)[b]

[a]M_n of PS graft on NCT particles. [b]Number of THY groups per particle estimated from the prior literature.[38]

similar recognition group density (1 DAP group per ~4.0 to 4.5 kDa polymer), except when treating DAP group density as a variable, in which case the system is marked with an asterisk (e.g., LPS-8*).

DAP-modified polymers were added to thymine-modified NCT particles (THY−NCT, 18 nm gold nanoparticle cores; Figure 1b) in anisole, readily inducing aggregation via hydrogen bond formation. Samples were initially prepared by adjusting the concentration of THY−NCTs and DAP−polymers such that the total number of polymer-bound DAP groups and particle-bound THY groups in the system were equal. The thermal stability and structure of the assemblies were investigated through variable temperature UV−vis spectroscopy (Figure 2). As the temperature increased, dissociation of NCT crystallites resulted in increasing absorbance at 520 nm from unbound particles, which exhibit a strong blue-shifted plasmonic response compared with assembled particles.[38]

For polymer systems at a fixed grafting density of DAP groups, increasing polymer binder length (and hence the number of DAP groups per chain) led to greater thermal stability of the polymer−NCT assemblies, even though each system contained the same total number of DAP and THY groups (Figure 2a). Furthermore, assemblies made with the lower-grafting density LPS-8* had a melting temperature below LPS-12 despite having the same polymer backbone with fewer DAP groups to bind per chain. These results indicate that multivalent binding strength is not a summation of individual bonds but rather suggests a complex role for the topology of the multivalent scaffold in determining the collective thermodynamics of binding.

Multivalency Number and Polymer Architecture. To more quantitatively examine how scaffold design affects supramolecular multivalency in these systems, van't Hoff plots were used to determine the enthalpy (ΔH_{NCT}) and entropy (ΔS_{NCT}) of polymer−NCT assemblies (see Supporting Information for details of these calculations). Normalizing ΔH_{NCT} by the enthalpy of a single complex ($\Delta H_{DAP-THY}$) allows for the calculation of the multivalency number, N (eq 1).

$$N = \frac{\Delta H_{NCT}}{\Delta H_{DAP-THY}} \quad (1)$$

By definition, the multivalency number N is the number of supramolecular bonds that act as a collective unit.[44] Prior work theorized that N directly correlates to the number of supramolecular groups in a "bundle", representing the maximum number of supramolecular groups able to be localized in a small volume.[18] In the "brick and mortar" assembly system used here, we hypothesized that polymer

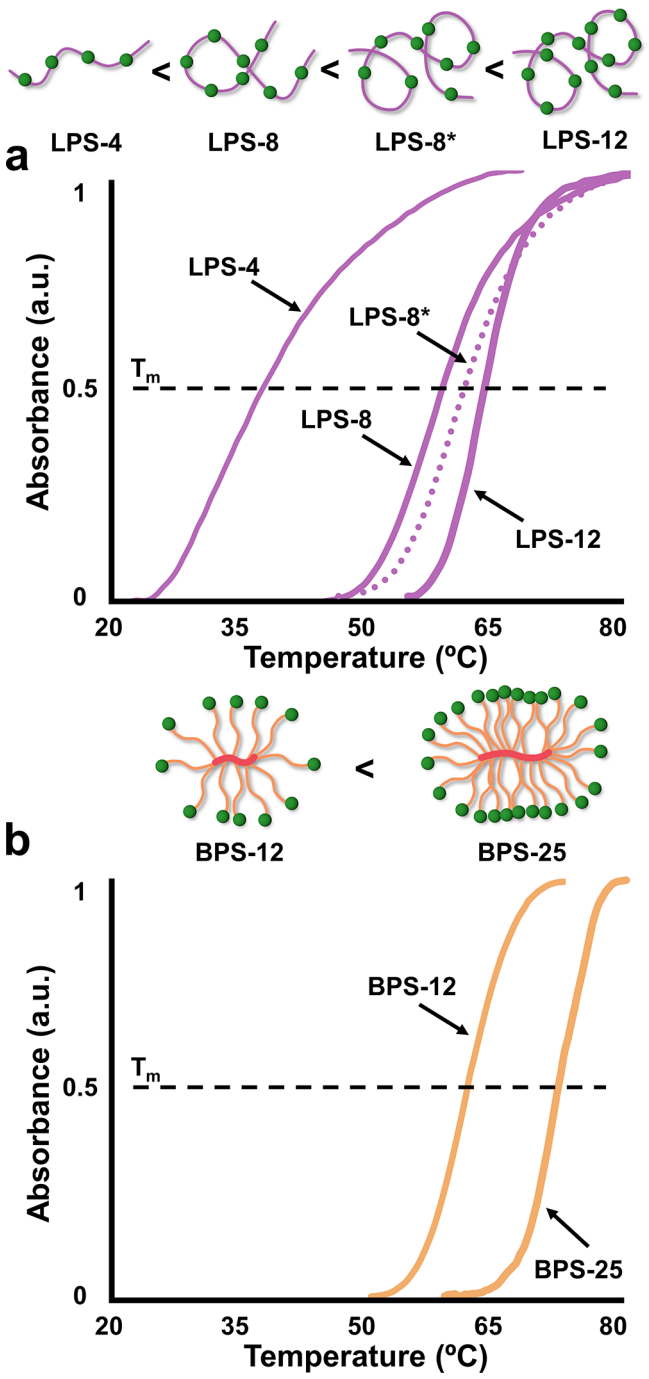

Figure 2. Thermodynamic stability of polymer−NCT crystals. (a, b) Absorbance measurements of colloidal polymer−NCT solutions as a function of temperature for (a) linear and (b) brush polymer binders.

binders (which constrain the distribution of DAP groups along the polymer backbone) would act as bundling agents that define the volume within which bond exchange can freely occur. Thus, polymer binder design could directly control both N and the entropic penalty paid upon binding, thereby dictating the thermodynamic behavior. While this bundling effect is conceptually similar to sticker aggregation observed in supramolecular polymer systems, the thermodynamic stability of a bundle in this system is not being altered by the formation of nanophase-separated domains, but rather the reassociation and exchange of transient bonds within a localized volume.[22,23]

https://doi.org/10.1021/jacs.4c02617
J. Am. Chem. Soc. 2024, 146, 11532−11541

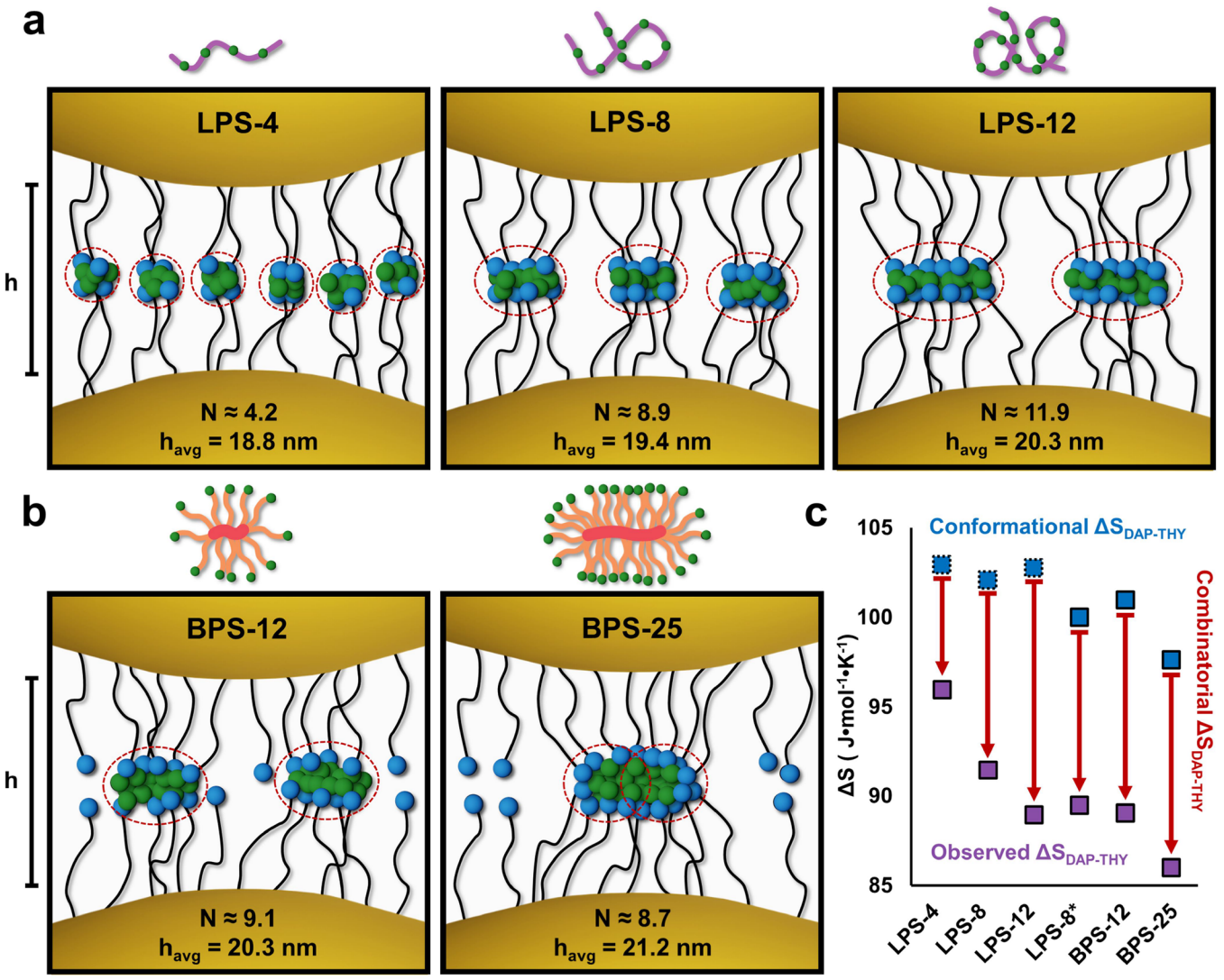

Figure 3. Multivalent behaviors of polymer–NCTs. (a) Linear polymer–NCTs were found to possess multivalency numbers (N) corresponding to the number of recognition groups per polymer chain. Representative bundles (effective exchange volumes) are depicted with dashed red outlines. (b) Brush polymer–NCTs displayed N values lower than the number of recognition groups per polymer chain. Representative bundles (effective exchange volumes) are depicted with dashed red outlines. (c) Combining the measured entropic loss of binding with a modeled combinatorial entropy, both normalized by effective valency, revealed the degree to which multivalency contributes to the total entropic efficiency for each system.

The simplest comparison of polymer binders' effects on multivalency is between linear polymer systems LPS-4, LPS-8, and LPS-12 (Figure 3a). These systems used the same THY–NCTs, contained the same total number of DAP groups, and kept the ratio of DAP groups to polymer mass constant, such that the only differences were the length of polymer chains and the number of DAP groups per polymer. In these assemblies, a direct correlation between the multivalency number N and the number of DAP recognition sites per chain was observed (i.e., $N \sim 4/8/12$ for LPS-4/8/12, respectively).

In contrast, the relatively constrained brush polymer systems exhibit multivalency numbers lower than the number of DAP groups per polymer (Figure 3b). This indicates that either brush polymers are unable to adopt conformations that permit all DAPs to be simultaneously bound or that DAP groups are unable to act coordinatively across the entire length of a brush polymer. We hypothesize that the difference in multivalency trends for LPS and BPS systems is related to their nanoscale topology.[20] Linear polymers adopt globular conformations with large degrees of configurational freedom, enabling each DAP group along a polymer's backbone to freely exchange with available THY groups at the NCT–NCT interface. Conversely, the steric bulk of the macromolecular brushes limits the segmental motion and restricts their conformation space. Prior work has shown that chain ends can become too separated to readily exchange in larger bottlebrush polymer architectures,[45] and this inability for end groups at distant points on the bottlebrush polymer to colocalize could explain why the multivalency number of BPS binders was lower than the total number of DAP groups per bottlebrush. Thus, larger brush polymer binders may contribute to more than one multivalent bundle on average.

To explain why BPS binders exhibit relatively higher melting temperatures than LPS binders, despite lower multivalency numbers (and hence lower ΔH_{NCT}), the binding entropy of the multivalent systems must be considered. Unlike enthalpy, however, ΔS_{NCT} cannot be accurately represented by a linear

https://doi.org/10.1021/jacs.4c02617
J. Am. Chem. Soc. 2024, 146, 11532–11541

sum of individual bond contributions, as it exhibits a more complicated relationship to the multivalent binder structure.

We hypothesize two primary entropic contributions within a bundle, both controllable by the polymer binder design. The first is a conformational entropy penalty that is paid when DAP and THY groups bind, arising from the restricted motion of the attached polymer chains. This entropic penalty from reduced polymer conformations is counterbalanced by an entropic gain unique to multivalent systems, stemming from the combinatorial nature of multivalent interactions.[46] Specifically, because each polymer and NCT scaffold possesses many DAP or THY groups that can freely exchange, there are multiple possible pairwise configurations of supramolecular groups within a multivalent bundle. Sometimes described as an "avidity entropy", this combinatorial component has a degeneracy which increases with the multivalency number N and scales according to eq 2.[47]

$$\Omega = \frac{n!m!}{(n-i)!(m-i)!i!} \tag{2}$$

Here, n is the number of DAP groups in a bundle, m is the number of THY units available to bind, and i is the number of bound pairs. In the simplifying but representative case where $n = m = i$ (all sites are matched and bound) and the entropy is taken as $\Delta S = R\ln(\Omega)$, the combinatorial entropy can be calculated as

$$\Delta S_{\mathrm{Comb}} = R\ln(N!) \tag{3}$$

Calculating ΔS_{Comb} makes it possible to determine the monovalent entropy loss in forming a single DAP−THY complex in the system, which we take to represent the conformational entropy of binding (ΔS_{Conf}):

$$\Delta S_{\mathrm{Conf}} = \frac{\Delta S_{\mathrm{NCT}} - \Delta S_{\mathrm{Comb}}}{N} \tag{4}$$

The observed valency adjusted entropy to bind $\Delta S_{\mathrm{DAP-THY}}$ (Figure 3c, purple data) is a summation of the conformational entropy penalty and the combinatorial entropy benefit. Because these two effects counterbalance one another, it is helpful to consider how trends in multivalency (reflected in ΔS_{Comb}) and backbone architecture (reflected in $\Delta S_{\mathrm{DAP-THY}}$) affect the overall system behavior as the multivalent scaffold design is altered. For example, systems with the same density of DAP groups (LPS-4, LPS-8, and LPS-12) exhibit conformational entropies that are largely equal (Figure 3c, dashed blue boxes). This parity in conformational penalty, likely aided by differences in particle separation (h) as determined by small-angle X-ray scattering (SAXS, Figure S8), suggests that variation in entropic efficiency can be entirely attributed to differences in multivalency between these systems. Conversely, LPS-8* and LPS-12 have comparable observed entropy values, but the lower conformational entropy penalty of LPS-8* indicates that entropic efficiency arises from this lower density scaffold being pinned by fewer DAP−THY binding events, giving it greater conformational freedom. Similarly, while BPS systems have stunted multivalency numbers compared to LPS-12 (and thus lower combinatorial entropy), their overall binding strength remained high because their conformational entropy to bind was, as expected, low compared to LPS systems.

These findings provide multiple handles for material designers to engineer the thermodynamics of massive multivalent assemblies. The conformational entropy can be modified via functional group density and backbone architecture, while the combinatorial entropy (as dictated through the multivalency number) can be adjusted via the number and configurational freedom of supramolecular groups on a chain. These handles show complex but rationally describable behavioral trends explained by the capacity of polymer binders to form nanoscale bundles. Thus, a systems level approach to materials design that considers the distribution of supramolecular units at multiple length scales (and how this distribution is affected by the size and shape of the scaffold) can be exploited to alter assembly thermodynamics in a sophisticated manner.

Role of Stoichiometry in Polymer−NCT Assembly. The investigations above compared systems where the total number of DAP and THY groups in each assembly was kept equivalent, but further control of multivalent thermodynamics can be achieved via off-stoichiometric combinations. The effects of changing assembly stoichiometry are not necessarily obvious, however, as the complexity of bundling behaviors can give rise to highly local stoichiometric deviations. To evaluate these potential effects, combinations with a range of polymer:NCT stoichiometries were prepared, from DAP−polymer deficient (DAP:THY = 0.1) to DAP−polymer abundant (DAP:THY = 20).

For all systems, increasing the amount of polymer binder (i.e., increasing total DAP:THY ratio) increased thermal stability (Figure 4). This suggests that multivalent polymer binders, unlike small molecules, do not exert significant competitive binding pressure.[7] It is also notable that this stoichiometry-dependent behavior is not exhibited with direct NCT−NCT systems (Figure 4c). We hypothesize that these stoichiometric effects arise because of the intermediate size of the polymer binders in this "brick and mortar" design. On one hand, the polymer binders are larger and sterically hindered compared to small molecules and thus tend to not compete with one another due to excluded volume effects. However, they are far smaller than NCTs and free to diffuse across NCT−NCT interfaces, thereby permitting greater clustering of recognition groups (i.e., larger bundles of supramolecular bonds) or reduced entropic penalties to form similar sized groupings.

Greater mechanistic clarity of bundling behaviors was provided through van't Hoff analysis to determine multivalency numbers and entropic efficiencies, and through SAXS to examine changes in interparticle distances (Figures 5 and S9). For LPS systems, increasing DAP:THY stoichiometry decreased the valency adjusted entropic penalty to bind ($\Delta S_{\mathrm{NCT}}/N$), while the multivalency number plateaued and interparticle spacing remained consistent (Figure 5a). Conversely, increasing the DAP:THY ratio in BPS systems continuously increased both lattice spacing and multivalency across the entire range of stoichiometries tested, with mirrored decreases in $\Delta S_{\mathrm{NCT}}/N$ (Figure 5b). Thus, even though both the linear and brush polymer binders exhibited positive correlations between melting temperatures and amount of binder added, these differences indicate that the mechanisms behind those increases must be distinct.

Linear polymers naturally adopt coiled conformations, and thus should have their largest recognition group density near their center (Figure 5a).[48] We therefore hypothesize that for linear binders, cooperative bundling between DAP groups on separate chains is effectively prevented by steric hindrance, and

https://doi.org/10.1021/jacs.4c02617
J. Am. Chem. Soc. 2024, 146, 11532−11541

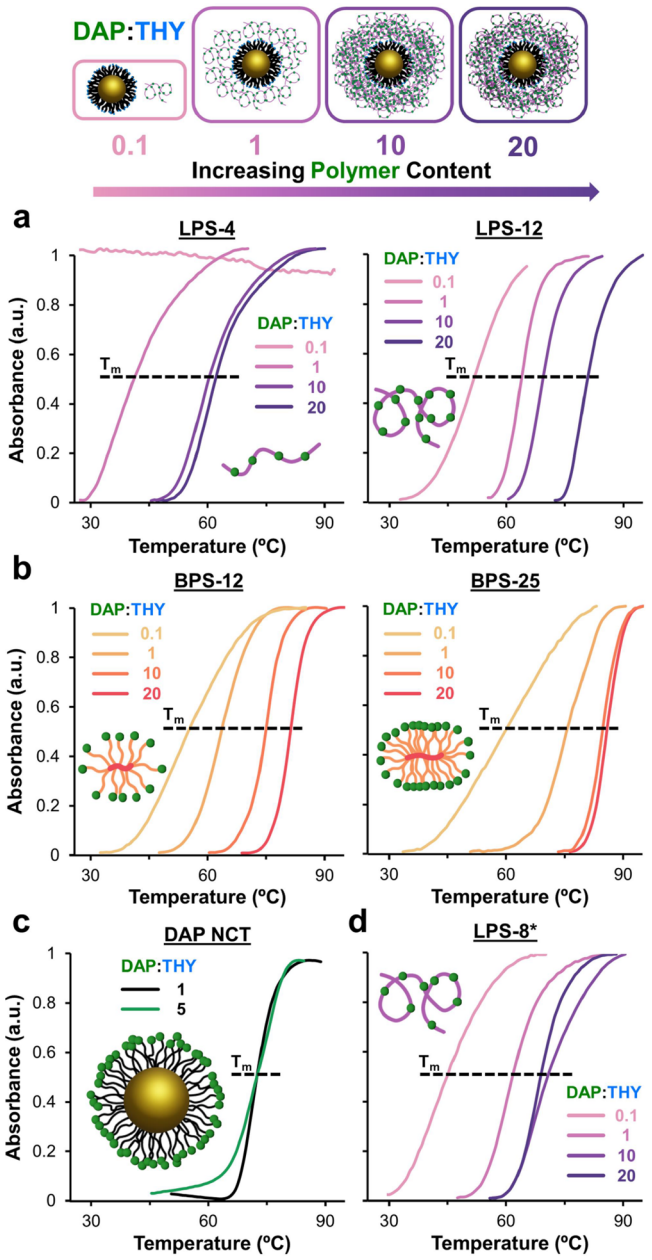

Figure 4. Thermal properties of polymer−NCTs with varying stoichiometry. (a, b) Melt curves of (a) linear and (b) brush polymer−NCTs showing increasing thermal stability as a function of the DAP:THY ratio. (c) Melt curves of particle-NCTs showing no dependence on concentration. (d) Melt curves of LPS-8* with the varying DAP:THY ratio showing saturation of thermal stability increases with an additional polymer binder.

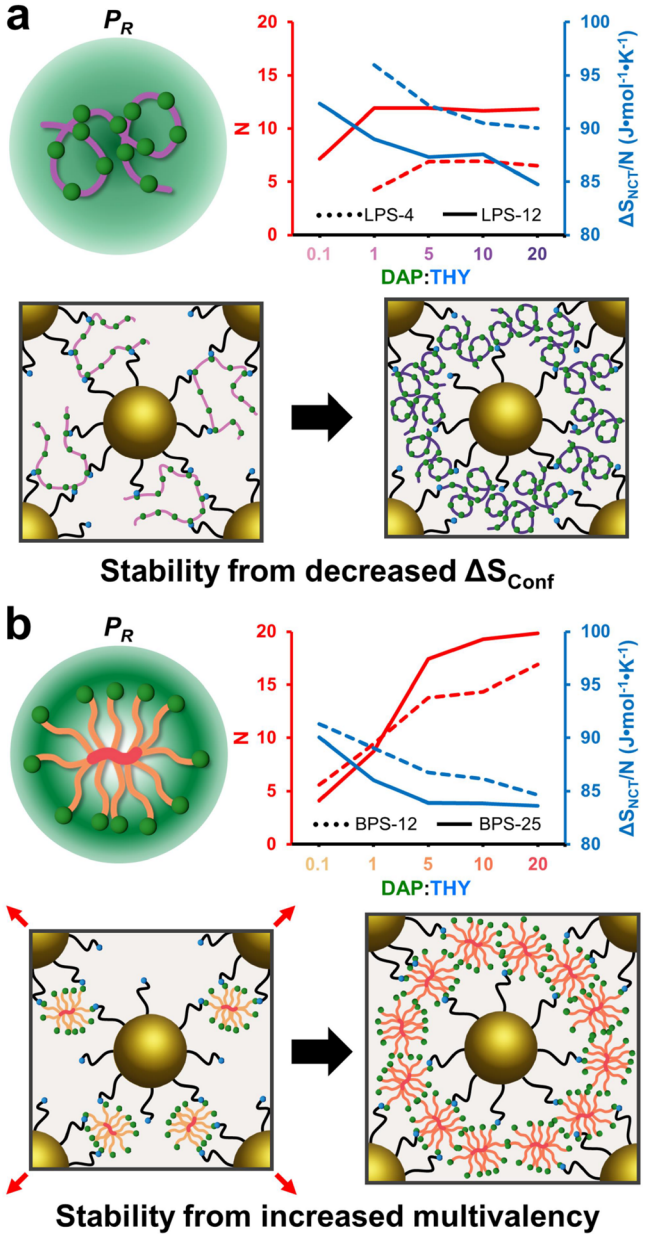

Figure 5. Thermodynamic analysis of polymer−NCTs varying stoichiometry. (a, b) Multivalency number (red) and valency normalized entropic costs (blue) of (a) linear and (b) brush polymer−NCT binding as a function of DAP:THY ratio with visualizations of recognition group probability density (P_R). The inner vs outer concentrations of recognition groups on linear and brush polymers, respectively, help explain the specific mechanisms by which each system increases thermal stability with increasing polymer presence.

thus improvements in entropic efficiency with increasing scaffold concentrations are driven by reduced conformational entropy penalties. Brush polymers, however, tend to have recognition groups positioned at the outer edges of their occupied volume because of crowding effects arising from the brush architecture (Figure 5b).[49] This structure can facilitate cooperative bundling between separate chains, meaning that increasing the concentration of BPS binders at the NCT−NCT interface could facilitate bundles that share DAP groups with adjacent bottlebrushes. These multibinder bundles would increase multivalency and hence improve entropic efficiency via higher combinatorial entropy gains. This hypothesis is supported by the values of N in the BPS-12 system, which go well above 12 (the number of DAP groups on a single BPS-12 polymer). These results highlight how the interplay of organizational constraints on supramolecular groups across both nanoscale scaffolds and mesoscale interfaces can affect assembly behaviors, further emphasizing the need for a systems-level understanding of supramolecular thermodynamics in massively multivalent building blocks.

Meso-to-Micro Scale Morphology Control. The relationship between NCT assemblies' melting temperatures and the architecture of polymer scaffolds clearly demonstrates

https://doi.org/10.1021/jacs.4c02617
J. Am. Chem. Soc. 2024, 146, 11532−11541

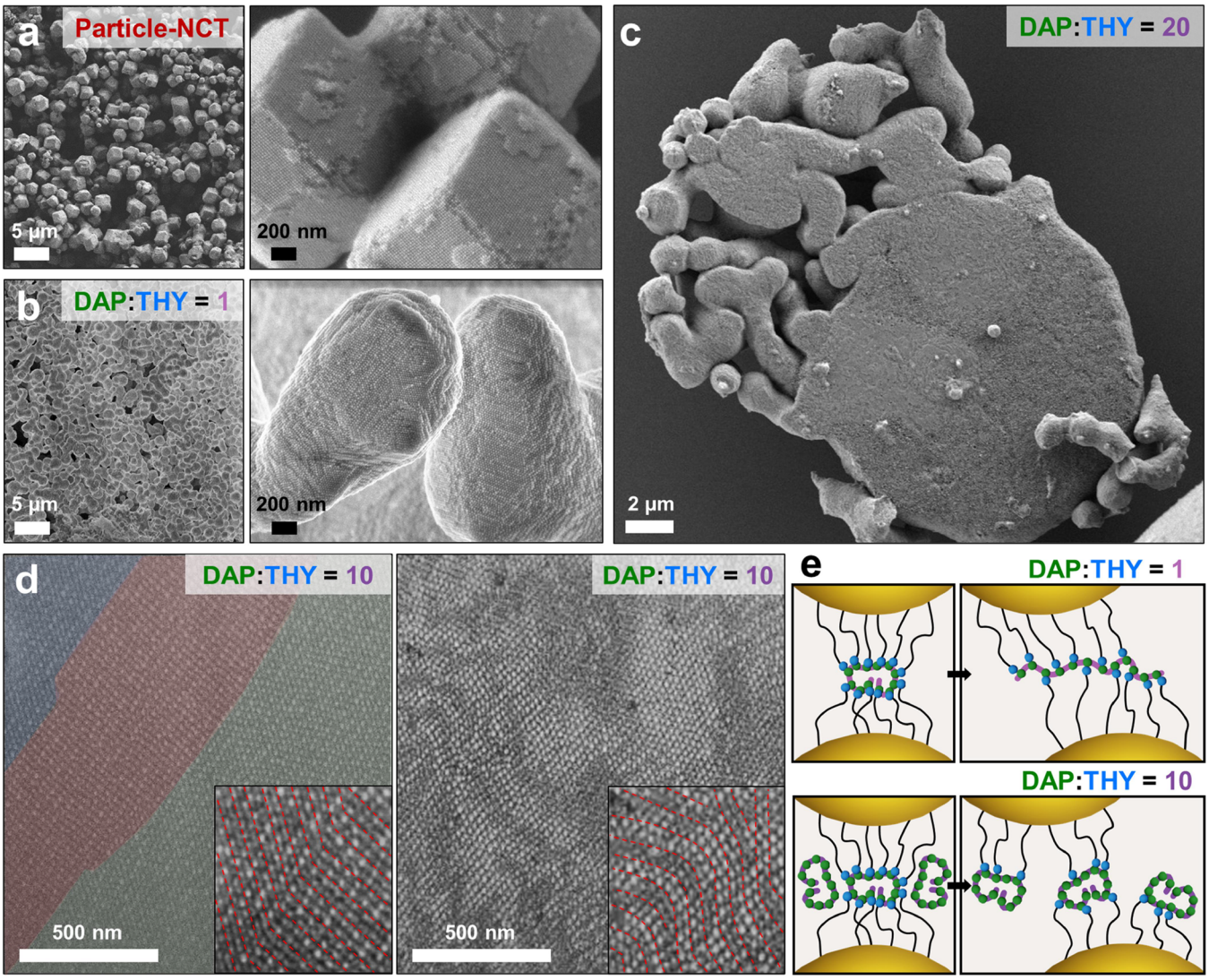

Figure 6. Morphological control in polymer−NCTs. (a−c) SEM images of crystallites formed from (a) BCC NCTs, made by directly combining DAP−NCT and THY−NCT particles, showing faceted Wulff-polyhedra, (b) polymer−NCTs made from LPS-12 at DAP:THY = 1, and (c) polymer NCTs made from LPS-12 at DAP:THY = 20. (d) Focused ion beam (FIB) milled cross sections showing polycrystalline grains (left) and paracrystalline distortion (right) between coalesced crystallites (dotted red lines in insets are a visual aid and do not necessarily represent crystallographic planes). (e) Diagram of LPS-12 polymer−NCT systems at DAP:THY = 1 and 10 responding to shear showing how excess polymer binder can facilitate slippage between NCTs.

that the nanoscale structure of a multivalent system can influence its thermodynamic behavior. While some indication was provided that it can also influence hierarchical organization (i.e., the changes in the NCT−NCT bond distance), it is important to demonstrate that these principles can also be used to manipulate the structure and behavior of the supramolecular system as a whole. Here, we demonstrate how multivalent polymer binders can alter the assembly and processing conditions of NCTs, thereby manipulating the meso- to microscale structural features of NCT-based superlattices.

Prior work on NCT assemblies using binary pairs of particles functionalized with either DAP or THY groups produced single-crystalline BCC superlattices when thermally annealed (Figure 6a).[38,41] The "brick and mortar" assembly strategy used here also produces high-quality NCT crystals. However, the crystallites exhibit FCC unit cells and typically do not have clear surface faceting as confirmed both in solution with SAXS, and by SEM after solvent removal (Figures S9 and 6b respectively). FCC structures are expected based on the results of comparable particle assemblies.[42] More specifically, when NCT−NCT bonding is mediated by a molecular species significantly smaller than an individual NCT, the assembly proceeds as if the particles are self-complementary, which tends to favor denser FCC packing. Additionally, prior work on colloidal superlattices showed that the lack of faceting in FCC structures occurs because the relative energies of different surface facets are too similar for any one facet to be the predominant product.[50] While this lack of surface faceting in FCC crystallites is unsurprising, these assemblies do possess unexpected microstructural features. Specifically, NCTs assembled with polymer binders tended to form connected collections of crystallites that indicate much more extensive crystallite-crystallite coalescence than observed in previous NCT superlattices (Figures 6b and S10). Importantly, the characteristic size of these crystals was sensitive to the

https://doi.org/10.1021/jacs.4c02617
J. Am. Chem. Soc. 2024, 146, 11532−11541

DAP:THY ratio. Crystallites formed in DAP:THY = 1 polymer−NCT systems were ∼0.8 μm in diameter (similar to particle-NCTs), while greater DAP:THY ratios produced crystallites that reached 10s−100s of micrometers in diameter (Figures 6c and S10). Focused ion-beam (FIB) cross sections of larger assemblies show long-range polycrystalline order with distinct grains and various orientations (Figure 6d, left), suggesting that the polymer-binder approach to NCT assembly promoted crystallite coalescence more than direct NCT−NCT binding.

We hypothesize that crystal−crystal fusion is enabled by the "brick and mortar" style of assembly because the more mobile polymer binders help facilitate the interfacial reorganization necessary to fuse crystallites without incurring a large entropic penalty from NCT brush distortion. This hypothesis is further supported by the presence of cross sections showing grains that lack clearly defined boundaries, instead showing waves of paracrystalline distortion, where the crystallographic planes shift direction in a continuous manner to accommodate the strain of lattice mismatch (Figure 6d, right). Notably, these distortions are not commonly observed in polycrystalline NCT assemblies formed by direct NCT−NCT bonding fused via extended centrifugation. This is because these distortions necessitate significant stretching or compression of the multivalent NCT brush scaffold, incurring a large entropy penalty. However, we hypothesize that excess polymer binders facilitate the reorganization of polymer−NCT assemblies as particles can easily slip past each other by exchanging supramolecular pairings to new binders (Figure 6e). Thus, the NCT superlattices rearrange into continuous solids to maximize the enthalpy of supramolecular binding without incurring a significant entropic penalty. This polymer-enabled consolidation therefore demonstrates how the scaffold structure in a multivalent system can tune structural features across mesoscale (paracrystalline distortion of crystal grains) and microscale (formation of large polycrystals) size regimes. Thus, in addition to rationally altering the thermodynamics of supramolecular binding, controlling the multivalent behavior of these systems can also enhance processability to permit control over hierarchical structure in these supramolecular materials.

CONCLUSIONS

Just as supramolecular chemistry provides a sort of "molecular masonry" by which structure can be programmed as a function of chemical interactions, massively multivalent building blocks can extend this programming to nano-, meso-, and microscale features by using a "brick and mortar" approach. We demonstrated this concept by using multivalent polymers to mediate emergent nanoscale bundling phenomena, thereby permitting control over the formation of larger structural features. The more sophisticated understanding of multivalent behaviors at nanoscale interfaces represents a significant advance toward the rational design of complex hierarchical materials. While this work focuses on the thermodynamics of assembly in synthetic model systems, it also has implications for fields which explore hierarchical organization in complex natural systems, such as catalysis, interface science, and biological inhibition.[27,51,52] We predict that further investigation using the design principles outlined here will utilize the architecture and composition of multivalent nanoscale scaffolds to further dictate exchange volumes and provide stimuli-responsive control of bundling behaviors. Such dynamic control of multivalency, especially when paired with in situ characterization of polymer behaviors, will enable novel assembly pathways, triggered reorganization of interfaces, and stabilized materials able to be processed into high-quality devices with nano-to-macroscale control of hierarchical structure.

ASSOCIATED CONTENT

Supporting Information

The Supporting Information is available free of charge at https://pubs.acs.org/doi/10.1021/jacs.4c02617.

Materials and instrumentation, synthetic protocols, characterization, and experimental details (PDF)

AUTHOR INFORMATION

Corresponding Author

Robert J. Macfarlane − *Department of Materials Science and Engineering, Massachusetts Institute of Technology, Cambridge, Massachusetts 02139, United States;* orcid.org/0000-0001-9449-2680; Email: rmacfarl@mit.edu

Authors

Carl J. Thrasher − *Department of Materials Science and Engineering, Massachusetts Institute of Technology, Cambridge, Massachusetts 02139, United States*

Fei Jia − *Department of Materials Science and Engineering, Massachusetts Institute of Technology, Cambridge, Massachusetts 02139, United States;* Present Address: Hangzhou Institute of Medicine (HIM), Chinese Academy of Sciences, Hangzhou 310022, China

Daryl W. Yee − *Department of Materials Science and Engineering, Massachusetts Institute of Technology, Cambridge, Massachusetts 02139, United States;* Present Address: Institute of Electrical and Micro Engineering École Polytechnique Fédérale de Lausanne, Neuchâtel 2000, Switzerland

Joshua M. Kubiak − *Department of Materials Science and Engineering, Massachusetts Institute of Technology, Cambridge, Massachusetts 02139, United States*

Yuping Wang − *Department of Materials Science and Engineering, Massachusetts Institute of Technology, Cambridge, Massachusetts 02139, United States;* Present Address: Stoddart Institute of Molecular Science, Department of Chemistry, Zhejiang University, Hangzhou 310027, China; Present Address: ZJU-Hangzhou Global Scientific and Technological Innovation Center, Hangzhou 311215, China

Margaret S. Lee − *Department of Materials Science and Engineering, Massachusetts Institute of Technology, Cambridge, Massachusetts 02139, United States;* orcid.org/0000-0003-0578-1427

Michika Onoda − *Department of Materials Science and Engineering, Massachusetts Institute of Technology, Cambridge, Massachusetts 02139, United States*

A. John Hart − *Department of Materials Science and Engineering, Massachusetts Institute of Technology, Cambridge, Massachusetts 02139, United States;* orcid.org/0000-0002-7372-3512

Complete contact information is available at: https://pubs.acs.org/10.1021/jacs.4c02617

Author Contributions

[¶]C.J.T. and F.J. contributed equally. All authors have given approval to the final version of the manuscript.

Notes

The authors declare no competing financial interest.

■ ACKNOWLEDGMENTS

This work was supported with funding from the National Science Foundation (Macromolecular, Supramolecular, and Nanochemistry, Award CHE-2304909). It was also supported by funding from the Department of the Navy, Office of Naval Research, under ONR Award N00014-22-1-2148 and by a Department of Defense MURI Award N00014-23-1-2499. Research was sponsored by the U.S. Army Research Office and U.S. Army Research Laboratory and was accomplished under Cooperative Agreement Number W911NF-23-2-0101. The views and conclusions contained in this document are those of the authors and should not be interpreted as representing the official policies, either expressed or implied, of the Army Research Office, Army Research Laboratory, or the U.S. Government. The U.S. Government is authorized to reproduce and distribute reprints for Government purposes notwithstanding any copyright notation hereon.

■ REFERENCES

(1) Fasting, C.; Schalley, C. A.; Weber, M.; Seitz, O.; Hecht, S.; Koksch, B.; Dernedde, J.; Graf, C.; Knapp, E.-W.; Haag, R. Multivalency as a Chemical Organization and Action Principle. *Angew. Chem., Int. Ed.* **2012**, *51* (42), 10472−10498.

(2) Boal, A. K.; Rotello, V. M. Fabrication and Self-Optimization of Multivalent Receptors on Nanoparticle Scaffolds. *J. Am. Chem. Soc.* **2000**, *122* (4), 734−735.

(3) Cheng, H. F.; Wang, S.; Mirkin, C. A. Electron-Equivalent Valency through Molecularly Well-Defined Multivalent DNA. *J. Am. Chem. Soc.* **2021**, *143* (4), 1752−1757.

(4) Girard, M.; Wang, S.; Du, J. S.; Das, A.; Huang, Z.; Dravid, V. P.; Lee, B.; Mirkin, C. A.; Olvera de la Cruz, M. Particle Analogs of Electrons in Colloidal Crystals. *Science* **2019**, *364* (6446), 1174−1178.

(5) Wang, S.; Lee, S.; Du, J. S.; Partridge, B. E.; Cheng, H. F.; Zhou, W.; Dravid, V. P.; Lee, B.; Glotzer, S. C.; Mirkin, C. A. The Emergence of Valency in Colloidal Crystals through Electron Equivalents. *Nat. Mater.* **2022**, *21* (5), 580−587.

(6) Markin, C. J.; Xiao, W.; Spyracopoulos, L. Mechanism for Recognition of Polyubiquitin Chains: Balancing Affinity through Interplay between Multivalent Binding and Dynamics. *J. Am. Chem. Soc.* **2010**, *132* (32), 11247−11258.

(7) Huskens, J.; Mulder, A.; Auletta, T.; Nijhuis, C. A.; Ludden, M. J. W.; Reinhoudt, D. N. A Model for Describing the Thermodynamics of Multivalent Host−Guest Interactions at Interfaces. *J. Am. Chem. Soc.* **2004**, *126* (21), 6784−6797.

(8) Badjić, J. D.; Nelson, A.; Cantrill, S. J.; Turnbull, W. B.; Stoddart, J. F. Multivalency and Cooperativity in Supramolecular Chemistry. *Acc. Chem. Res.* **2005**, *38* (9), 723−732.

(9) Gestwicki, J. E.; Cairo, C. W.; Strong, L. E.; Oetjen, K. A.; Kiessling, L. L. Influencing Receptor−Ligand Binding Mechanisms with Multivalent Ligand Architecture. *J. Am. Chem. Soc.* **2002**, *124* (50), 14922−14933.

(10) Ooi, H. W.; Kocken, J. M. M.; Morgan, F. L. C.; Malheiro, A.; Zoetebier, B.; Karperien, M.; Wieringa, P. A.; Dijkstra, P. J.; Moroni, L.; Baker, M. B. Multivalency Enables Dynamic Supramolecular Host−Guest Hydrogel Formation. *Biomacromolecules* **2020**, *21* (6), 2208−2217.

(11) Onoda, M.; Jia, F.; Takeoka, Y.; Macfarlane, R. J. Controlling the Dynamics of Elastomer Networks with Multivalent Brush Architectures. *Soft Matter* **2022**, *18* (19), 3644−3648.

(12) Yin, Y.; Dong, Z.; Luo, Q.; Liu, J. Biomimetic Catalysts Designed on Macromolecular Scaffolds. *Prog. Polym. Sci.* **2012**, *37* (11), 1476−1509.

(13) Hooper, J.; Liu, Y.; Budhadev, D.; Ainaga, D. F.; Hondow, N.; Zhou, D.; Guo, Y. Polyvalent Glycan Quantum Dots as a Multifunctional Tool for Revealing Thermodynamic, Kinetic, and Structural Details of Multivalent Lectin−Glycan Interactions. *ACS Appl. Mater. Interfaces* **2022**, *14* (42), 47385−47396.

(14) Reczek, J. J.; Kennedy, A. A.; Halbert, B. T.; Urbach, A. R. Multivalent Recognition of Peptides by Modular Self-Assembled Receptors. *J. Am. Chem. Soc.* **2009**, *131* (6), 2408−2415.

(15) de laRica, R.; Fratila, R. M.; Szarpak, A.; Huskens, J.; Velders, A. H. Multivalent Nanoparticle Networks as Ultrasensitive Enzyme Sensors. *Angew. Chem., Int. Ed.* **2011**, *50* (25), 5704−5707.

(16) Jin, Z.; Chen, T.; Liu, Y.; Feng, W.; Chen, L.; Wang, C. Multivalent Design of Low-Entropy-Penalty Ion−Dipole Interactions for Dynamic Yet Thermostable Supramolecular Networks. *J. Am. Chem. Soc.* **2023**, *145* (6), 3526−3534.

(17) Zhao, H.; Sen, S.; Udayabhaskararao, T.; Sawczyk, M.; Kučanda, K.; Manna, D.; Kundu, P. K.; Lee, J.-W.; Král, P.; Klajn, R. Reversible Trapping and Reaction Acceleration within Dynamically Self-Assembling Nanoflasks. *Nat. Nanotechnol.* **2016**, *11* (1), 82−88.

(18) Santos, P. J.; Cao, Z.; Zhang, J.; Alexander-Katz, A.; Macfarlane, R. J. Dictating Nanoparticle Assembly via Systems-Level Control of Molecular Multivalency. *J. Am. Chem. Soc.* **2019**, *141* (37), 14624−14632.

(19) Vonnemann, J.; Liese, S.; Kuehne, C.; Ludwig, K.; Dernedde, J.; Böttcher, C.; Netz, R. R.; Haag, R. Size Dependence of Steric Shielding and Multivalency Effects for Globular Binding Inhibitors. *J. Am. Chem. Soc.* **2015**, *137* (7), 2572−2579.

(20) Bhatia, S.; Camacho, L. C.; Haag, R. Pathogen Inhibition by Multivalent Ligand Architectures. *J. Am. Chem. Soc.* **2016**, *138* (28), 8654−8666.

(21) Mammen, M.; Choi, S.-K.; Whitesides, G. M. Polyvalent Interactions in Biological Systems: Implications for Design and Use of Multivalent Ligands and Inhibitors. *Angew. Chem., Int. Ed.* **1998**, *37* (20), 2754−2794.

(22) Nébouy, M.; Morthomas, J.; Fusco, C.; Chazeau, L.; Jabbari-Farouji, S.; Baeza, G. P. Mechanistic Understanding of Sticker Aggregation in Supramolecular Polymers: Quantitative Insights from the Plateau Modulus of Triblock Copolymers. *Macromolecules* **2022**, *55* (21), 9558−9570.

(23) Jangizehi, A.; Ahmadi, M.; Seiffert, S. Emergence, Evidence, and Effect of Junction Clustering in Supramolecular Polymer Materials. *Mater. Adv.* **2021**, *2* (5), 1425−1453.

(24) Walker, D. A.; Leitsch, E. K.; Nap, R. J.; Szleifer, I.; Grzybowski, B. A. Geometric Curvature Controls the Chemical Patchiness and Self-Assembly of Nanoparticles. *Nat. Nanotechnol.* **2013**, *8* (9), 676−681.

(25) Spratt, J.; Dias, J. M.; Kolonelou, C.; Kiriako, G.; Engström, E.; Petrova, E.; Karampelias, C.; Cervenka, I.; Papanicolaou, N.; Lentini, A.; Reinius, B.; Andersson, O.; Ambrosetti, E.; Ruas, J. L.; Teixeira, A. I. Multivalent Insulin Receptor Activation Using Insulin−DNA Origami Nanostructures. *Nat. Nanotechnol.* **2023**, *19*, 237.

(26) Du, R. R.; Cedrone, E.; Romanov, A.; Falkovich, R.; Dobrovolskaia, M. A.; Bathe, M. Innate Immune Stimulation Using 3D Wireframe DNA Origami. *ACS Nano* **2022**, *16* (12), 20340−20352.

(27) Veneziano, R.; Moyer, T. J.; Stone, M. B.; Wamhoff, E.-C.; Read, B. J.; Mukherjee, S.; Shepherd, T. R.; Das, J.; Schief, W. R.; Irvine, D. J.; Bathe, M. Role of Nanoscale Antigen Organization on B-Cell Activation Probed Using DNA Origami. *Nat. Nanotechnol.* **2020**, *15* (8), 716−723.

(28) Wang, M.; Yang, D.; Lu, Q.; Liu, L.; Cai, Z.; Wang, Y.; Wang, H.-H.; Wang, P.; Nie, Z. Spatially Reprogramed Receptor Organization to Switch Cell Behavior Using a DNA Origami-Templated Aptamer Nanoarray. *Nano Lett.* **2022**, *22* (21), 8445−8454.

(29) Liu, Y.; Wijesekara, P.; Kumar, S.; Wang, W.; Ren, X.; Taylor, R. E. The Effects of Overhang Placement and Multivalency on Cell Labeling by DNA Origami. *Nanoscale* **2021**, *13* (14), 6819−6828.
(30) Jones, M. R.; Macfarlane, R. J.; Prigodich, A. E.; Patel, P. C.; Mirkin, C. A. Nanoparticle Shape Anisotropy Dictates the Collective Behavior of Surface-Bound Ligands. *J. Am. Chem. Soc.* **2011**, *133* (46), 18865.
(31) Xia, Y.; Nguyen, T. D.; Yang, M.; Lee, B.; Santos, A.; Podsiadlo, P.; Tang, Z.; Glotzer, S. C.; Kotov, N. A. Self-Assembly of Self-Limiting Monodisperse Supraparticles from Polydisperse Nanoparticles. *Nat. Nanotechnol.* **2011**, *6* (9), 580−587.
(32) Vial, S.; Nykypanchuk, D.; Yager, K. G.; Tkachenko, A. V.; Gang, O. Linear Mesostructures in DNA−Nanorod Self-Assembly. *ACS Nano* **2013**, *7* (6), 5437−5445.
(33) Thaner, R. V.; Kim, Y.; Li, T. I. N. G.; Macfarlane, R. J.; Nguyen, S. T.; Olvera de la Cruz, M.; Mirkin, C. A. Entropy-Driven Crystallization Behavior in DNA-Mediated Nanoparticle Assembly. *Nano Lett.* **2015**, *15* (8), 5545−5551.
(34) Li, R. L.; Thrasher, C. J.; Hueckel, T.; Macfarlane, R. J. Hierarchically Structured Nanocomposites via a "Systems Materials Science" Approach. *Acc. Mater. Res.* **2022**, *3*, 1248.
(35) Boal, A. K.; Gray, M.; Ilhan, F.; Clavier, G. M.; Kapitzky, L.; Rotello, V. M. Bricks and Mortar Self-Assembly of Nanoparticles. *Tetrahedron* **2002**, *58* (4), 765−770.
(36) Boal, A. K.; Galow, T. H.; Ilhan, F.; Rotello, V. M. Binary and Ternary Polymer-Mediated "Bricks and Mortar" Self-Assembly of Gold and Silica Nanoparticles. *Adv. Funct. Mater.* **2001**, *11* (6), 461−465.
(37) Boal, A. K.; Ilhan, F.; DeRouchey, J. E.; Thurn-Albrecht, T.; Russell, T. P.; Rotello, V. M. Self-Assembly of Nanoparticles into Structured Spherical and Network Aggregates. *Nature* **2000**, *404* (6779), 746−748.
(38) Zhang, J.; Santos, P. J.; Gabrys, P. A.; Lee, S.; Liu, C.; Macfarlane, R. J. Self-Assembling Nanocomposite Tectons. *J. Am. Chem. Soc.* **2016**, *138* (50), 16228.
(39) Wang, Y.; Santos, P. J.; Kubiak, J. M.; Guo, X.; Lee, M. S.; Macfarlane, R. J. Multistimuli Responsive Nanocomposite Tectons for Pathway Dependent Self-Assembly and Acceleration of Covalent Bond Formation. *J. Am. Chem. Soc.* **2019**, *141* (33), 13234−13243.
(40) Santos, P. J.; Macfarlane, R. J. Reinforcing Supramolecular Bonding with Magnetic Dipole Interactions to Assemble Dynamic Nanoparticle Superlattices. *J. Am. Chem. Soc.* **2020**, *142* (3), 1170.
(41) Santos, P. J.; Gabrys, P. A.; Zornberg, L. Z.; Lee, M. S.; Macfarlane, R. J. Macroscopic Materials Assembled from Nanoparticle Superlattices. *Nature* **2021**, *591* (7851), 586−591.
(42) Yee, D. W.; Lee, M. S.; An, J.; Macfarlane, R. J. Reversible Diffusionless Phase Transitions in 3D Nanoparticle Superlattices. *J. Am. Chem. Soc.* **2023**, *145* (11), 6051−6056.
(43) Santos, P. J.; Cheung, T. C.; Macfarlane, R. J. Assembling Ordered Crystals with Disperse Building Blocks. *Nano Lett.* **2019**, *19* (8), 5774−5780.
(44) Jin, R.; Wu, G.; Li, Z.; Mirkin, C. A.; Schatz, G. C. What Controls the Melting Properties of DNA-Linked Gold Nanoparticle Assemblies? *J. Am. Chem. Soc.* **2003**, *125* (6), 1643.
(45) Jia, F.; Song, J.; Kubiak, J. M.; Onoda, M.; Santos, P. J.; Sano, K.; Holten-Andersen, N.; Zhang, K.; Macfarlane, R. J. Brush Polymers as Nanoscale Building Blocks for Hydrogel Synthesis. *Chem. Mater.* **2021**, *33* (14), 5748−5756.
(46) Martinez-Veracoechea, F. J.; Leunissen, M. E. The Entropic Impact of Tethering, Multivalency and Dynamic Recruitment in Systems with Specific Binding Groups. *Soft Matter* **2013**, *9* (12), 3213−3219.
(47) Kitov, P. I.; Bundle, D. R. On the Nature of the Multivalency Effect: A Thermodynamic Model. *J. Am. Chem. Soc.* **2003**, *125* (52), 16271−16284.
(48) Heidari, M.; Labousse, M.; Leibler, L. Ordering of Functional Groups by Confining Grafted Chains, Star Polymers, or Polymer-Stabilized Nanoparticles. *Macromolecules* **2020**, *53* (10), 3907−3913.
(49) Murat, M.; Grest, G. S. Structure of a Grafted Polymer Brush: A Molecular Dynamics Simulation. *Macromolecules* **1989**, *22* (10), 4054−4059.
(50) Auyeung, E.; Li, T. I. N. G.; Senesi, A. J.; Schmucker, A. L.; Pals, B. C.; de la Cruz, M. O.; Mirkin, C. A. DNA-Mediated Nanoparticle Crystallization into Wulff Polyhedra. *Nature* **2014**, *505* (7481), 73−77.
(51) Alba-Molina, D.; Rodríguez-Padrón, D.; Puente-Santiago, A. R.; Giner-Casares, J. J.; Martín-Romero, M. T.; Camacho, L.; Martins, L. O.; Muñoz-Batista, M. J.; Cano, M.; Luque, R. Mimicking the Bioelectrocatalytic Function of Recombinant CotA Laccase through Electrostatically Self-Assembled Bioconjugates. *Nanoscale* **2019**, *11* (4), 1549−1554.
(52) Overeem, N. J.; Hamming, P. H. E.; Grant, O. C.; Di Iorio, D.; Tieke, M.; Bertolino, M. C.; Li, Z.; Vos, G.; de Vries, R. P.; Woods, R. J.; Tito, N. B.; Boons, G.-J. P. H.; van der Vries, E.; Huskens, J. Hierarchical Multivalent Effects Control Influenza Host Specificity. *ACS Cent. Sci.* **2020**, *6* (12), 2311−2318.

https://doi.org/10.1021/jacs.4c02617
J. Am. Chem. Soc. 2024, 146, 11532−11541